Biochemical and Biophysical Research Communications 433 (2013) 47–51

Contents lists available at SciVerse ScienceDirect

Biochemical and Biophysical Research Communications

journal homepage: www.elsevier.com/locate/ybbrc

Detection of early stage atherosclerotic plaques using PET and CT fusion imaging targeting P-selectin in low density lipoprotein receptor-deficient mice

Ikuko Nakamura [a,b], Koki Hasegawa [a,c], Yasuhiro Wada [a], Tetsuaki Hirase [b], Koichi Node [b], Yasuyoshi Watanabe [a,*]

[a] RIKEN Center for Molecular Imaging Science, Kobe, Japan
[b] Department of Cardiovascular Medicine, Saga University, Saga, Japan
[c] Department of Pathology and Experimental Medicine, Kumamoto University, Kumamoto, Japan

ARTICLE INFO

Article history:
Received 9 February 2013
Available online 26 February 2013

Keywords:
Atherosclerosis
PET
Molecular imaging
P-selectin

ABSTRACT

Background: Sensitive detection and qualitative analysis of atherosclerotic plaques are in high demand in cardiovascular clinical settings. The leukocyte–endothelial interaction mediated by an adhesion molecule P-selectin participates in arterial wall inflammation and atherosclerosis.
Methods and results: A ^{64}Cu-1,4,7,10-tetraazacyclododecane-1,4,7,10-tetraacetic acid conjugated anti-P-selectin monoclonal antibody (^{64}Cu-DOTA-anti-P-selectin mAb) probe was prepared by conjugating an anti-P-selectin monoclonal antibody with DOTA followed by ^{64}Cu labeling. Thirty-six hours prior to PET and CT fusion imaging, 3 MBq of ^{64}Cu-DOTA-anti-P-selectin mAb was intravenously injected into low density lipoprotein receptor-deficient *Ldlr*-/- mice. After a 180 min PET scan, autoradiography and biodistribution of ^{64}Cu-DOTA-anti-P-selectin monoclonal antibody was examined using excised aortas. In *Ldlr*-/- mice fed with a high cholesterol diet for promotion of atherosclerotic plaque development, PET and CT fusion imaging revealed selective and prominent accumulation of the probe in the aortic root. Autoradiography of aortas that demonstrated probe uptake into atherosclerotic plaques was confirmed by Oil red O staining for lipid droplets. In *Ldlr*-/- mice fed with a chow diet to develop mild atherosclerotic plaques, probe accumulation was barely detectable in the aortic root on PET and CT fusion imaging. Probe biodistribution in aortas was 6.6-fold higher in *Ldlr*-/- mice fed with a high cholesterol diet than in those fed with a normal chow diet. ^{64}Cu-DOTA-anti-P-selectin mAb accumulated selectively in aortic atherosclerotic plaques and was detectable by PET and CT fusion imaging in *Ldlr*-/- mice.
Conclusions: P-selectin is a candidate target molecule for early-phase detection by PET and CT fusion imaging of atherosclerotic plaques.

1. Introduction

Cardiovascular disease induced by atherosclerosis is a leading cause of death in the Western world. Coronary artery imaging based on morphological evaluation, including coronary angiography and multidetector-row CT, has largely contributed to the understanding of the pathophysiology of atherosclerosis and the prevention and treatment of coronary artery disease. The incidence of fatal acute coronary syndrome and of left ventricular dysfunction caused by coronary artery disease needs to be reduced [1]. Recent studies have revealed that the vulnerability of atherosclerotic plaques is an important determinant of initiation and progression of acute coronary syndrome. Accordingly, sensitive detection and qualitative analysis of atherosclerotic plaques are in high demand in the clinical setting.

Many studies have shown that chronic inflammation of the arterial wall is mediated by immune cells, and that inflammatory mediators play crucial roles in the pathogenesis of atherosclerosis [2]. In the initial step of arterial inflammation, the leukocyte–endothelial interaction mediated by endothelial cell adhesion molecules triggers leukocyte recruitment from the circulating blood into the arterial wall [3]. P-, E- and L-selectins, members of the selectin family, are calcium-dependent type-I transmembrane glycoproteins. They have extracellular lectin-like domains that bind carbohydrate ligands on leukocytes and participate in the initial capture, tethering and rolling along endothelial cells [4]. L-selectin is constitutively expressed by lymphocytes, and E-selectin is expressed by activated endothelial cells. P-selectin is stored in Weibel–Palade bodies of endothelial cells and is expressed in acute and chronically inflamed endothelium. P-selectin regulates the recruitment

* Corresponding author. Address: RIKEN Center for Molecular Imaging Science, 6-7-3, Minatojima-minamimachi, Chuo-ku, Kobe, Hyogo 650-0047, Japan. Fax: +81 78 304 7112.
E-mail addresses: nakamuri@riken.jp (I. Nakamura), yywata@riken.jp (Y. Watanabe).

0006-291X/$ - see front matter © 2013 Elsevier Inc. All rights reserved.
http://dx.doi.org/10.1016/j.bbrc.2013.02.069

of monocytes and lymphocytes, key players in arterial wall inflammation [5]. It was reported that P-selectin is expressed in human atherosclerotic plaques [6]. The facilitatory role of P-selectin in atherogenesis has been demonstrated with gene targeting using P-selectin-deficient mice [7].

Over the past decade, novel imaging techniques have been developed based on the growing understanding of the molecular mechanisms of diseases. PET imaging using antibody-based probes is a molecular imaging modality that can be used to detect molecular and cellular processes with high sensitivity and specificity [8]. In the present study, anti-P-selectin monoclonal antibody radiolabeled with ^{64}Cu via 1,4,7,10-tetraazacyclododecane-1,4,7,10-tetraacetic acid (DOTA) was prepared as a probe to target atherosclerotic plaques. PET and CT fusion imaging was then performed with the probe in atherosclerosis-prone low density lipoprotein receptor-deficient *Ldlr*-/- mice. Probe accumulation was then observed in atherosclerotic plaques by PET and CT fusion imaging. Autoradiography of dissected aortas and biodistribution studies after emission were then performed. The present results suggest that P-selectin is a candidate molecule that can be used to target atherosclerotic plaques with PET and CT fusion imaging.

2. Methods

2.1. Probe preparation

Anti-P-selectin monoclonal antibody (anti-P-selectin mAb) (Catalog Number 553741, BD Biosciences, San Jose, CA, USA) was conjugated with 1,4,7,10-tetraazacyclododecane-1,4,7,10-tetraacetic acid mono-*N*-hydroxysuccinimide ester (DOTA-NHS-ester) (Macrocyclics, Dallas, TX) as described previously [9]. Briefly, DOTA-NHS-ester was added to anti-P-selectin mAb (1 mg/mL) in phosphate-buffered saline (PBS) (Wako Pure Chemical Industries, Osaka, Japan) (molar ratios of DOTA-NHS-ester:anti-P-selectin mAb = 15:1) followed by incubation at room temperature for 4 h. Then, the mixture was purified by a PD-10 desalting column (GE Healthcare, Piscataway, NJ), and the eluted fraction was passed through an Amicon Ultra 4 filter (Millipore, Millerica, MA) to exchange the buffer from PBS to an acetate buffer. The resulting DOTA-anti-P-selectin mAb was stored at 4 °C. The average number of moles of DOTA attached per mole of anti-P-selectin was examined using laser desorption ionization time-of-flight mass spectrometry [10].

DOTA-anti-P-selectin mAb was radiolabeled with ^{64}Cu, according to a modified procedure described previously [11]. DOTA-anti-P-selectin mAb was incubated with ^{64}Cu-$CuCl_2$ at 40 °C for 1 h. The mixture was purified by Amicon ultra 0.5 columns. The affinity of ^{64}Cu-DOTA-anti-P-selectin mAb for P-selectin-IgG fusion protein (BD Biosciences) was examined using a 27 MHz quartz crystal microbalance (QCM) model Single Q (AS ONE Co. Osaka, Japan) [12]. P-selectin-IgG fusion protein in PBS (0.8 μg/mL) was immobilized on a QCM chamber for 30 min, and was then removed. After washing three times with PBS, 500 μL PBS containing bovine serum albumin (BSA) was added to the QCM chamber. ^{64}Cu-DOTA-anti-P-selectin mAb was added to the solution in the QCM chamber, and the change in resonance frequency was recorded. The mass of antibody binding on the sensor was determined from the oscillation frequency. The oscillation frequency change is correlated to the adsorbed mass (1 Hz = 30 pg). The binding affinity was indicated by frequency changes of the QCM, and the dissociation constant (K_d) was calculated with manufacturer developed software.

2.2. Animal studies

Two groups of male *Ldlr*-/- mice (The Jackson Laboratory, Bar Harbor, ME) were prepared. From 8 weeks of age, one group (n = 7) was fed with a high cholesterol diet (1.25% cholesterol, 7.5% cocoa butter, 7.5% casein; Harlan Laboratories, Inc., Indianapolis, IN) for 12 weeks in order to develop atherosclerosis lesions, and the other group (n = 7) was fed with normal chow (CE-2; CLEA Japan Inc., Tokyo, Japan). Mice were anesthetized for all procedures and imaged under inhalation anesthesia (1.5% isoflurane). All experimental protocols were approved by the Ethics Committee on Animal Care and Use of the Center for Molecular Imaging Science in RIKEN, and were performed in accordance with the Principles of Laboratory Animal Care (NIH publication No. 85-23, revised in 1985).

2.3. PET and CT imaging

PET scans were performed using a micro PET Focus220 (Siemens, Knoxville, TN). Thirty-six hours prior to PET imaging, three 2.84-3.37 MBq of ^{64}Cu-DOTA-P-selectin monoclonal antibody was intravenously injected into each mouse through a cannula in the tail vein. For anatomical reference, CT scan (Inveon CT, Siemens, Knoxville, TN) was performed after intravenously injecting 300 μL/body of Fenestra VC contrast agent (ART, Montreal, Canada). Following CT, mice were transferred to the PET scanner. PET data were acquired for 180 min. PET images were reconstructed with maximum a posteriori (MAP) with a Gibbs prior. The PET and CT images were co-registered using PMOD version 3.15 (PMOD Technologies, Zurich, Switzerland).

2.4. Autoradiography

Following PET imaging, the aorta was perfused with normal saline containing heparin (10 U/mL) under anesthesia. Then, the aortic samples from the middle of the left ventricle to the iliac bifurcation were dissected free from surrounding tissues, opened longitudinally, pinned onto a silicon-coated dish and stained with 0.5% Oil red O for 15 min at room temperature followed by a rinse with 60% (v/v) isopropanol for 5 min. After staining, the tissue was exposed for autoradiography on a Fuji FLA-7000 analyzer (Fuji Film, Tokyo, Japan) at a 25 μm resolution for 1 h (Fuji Film).

2.5. Biodistribution analysis

After autoradiography, the aorta was divided into two portions at the branching point of the subclavian artery, and the proximal portion was collected. Then, the aorta and other organs were recorded with a 1470 WIZARD Automatic Gamma Counter (PerkinElmer, Waltham, MA). Results adjusted for organ weight are expressed as means ± standard error (SE). Statistical significance was evaluated with the Mann–Whitney U test using DR.SPSS II for Windows (SPSS, Tokyo, Japan) for statistical analysis. p values smaller than 0.05 were considered statistically significant.

2.6. Microautoradiography

Microautoradiography was performed using a modified method reported previously [13]. Briefly, *Ldlr*-/- mice injected intravenously with ^{64}Cu-DOTA-anti-P-selectin mAb (10 MBq/mouse) were sacrificed at 16 h after administration. The excised aortas were embedded in Tissue-Tek OCT compound (Sakura Finetek Inc., Torrance, CA). Under a safety light, 5 μm-thick sections were created and mounted on slides coated with NTB2 nuclear emulsion (Kodak, Rochester, NY) diluted in 13:7 with distilled water. The slides were exposed in this way for 1 week, and then incubated in solutions of ethanol and acetic acid (19:1) at −70 °C and then 25 °C for 1 min each. After washing with water twice for 3 min, the sections were developed in D-19 developer (Kodak) for 5 min, fixed in Fuji Fix (Fuji Film) for 15 min at room temperature

and then washed in water for 10 min. After microautoradiography, the sections were subjected to hematoxylin and eosin (H&E) staining.

3. Results

3.1. PET and CT fusion imaging

The average number of DOTA chelator molecules was determined to be 2.5 per one anti-P-selectin mAb molecule. The specific radioactivity of ^{64}Cu-DOTA-P-selectin mAb was 0.7–1.3 GBq/mg. The dissociation constant (K_d) of ^{64}Cu-DOTA-anti-P-selectin mAb was 1.89 nM. *In vivo* CT with contrast was performed 30 min before PET for anatomical reference. CT enabled demonstration of the aorta and its major branches in mice. *In vivo* PET was performed 36 h after injection of ^{64}Cu-DOTA-anti-P-selectin mAb, the time referred and decided optimal from other mAb PET imagings in our laboratory. Accumulation of ^{64}Cu-DOTA-anti-P-selectin mAb was observed in the aortic root, aortic arch, and root of major branches identified by CT in *Ldlr*-/- mice fed with a high cholesterol diet (Fig. 1). In contrast, accumulation of ^{64}Cu-DOTA-anti-P-selectin mAb was barely detectable in the aortic tree in *Ldlr*-/- mice fed with normal chow that are resistant to atherosclerosis development (Fig. 1). Quantitative data calculated from the accumulated radioactivity of ^{64}Cu-DOTA-anti-P-selectin in aortic root were expressed as the target-to-muscle ratio. We set the region-of-interest (ROI) in the aortic arch and muscle. In addition, we set the ROI in intraventricular area to substract the radioactivity in the blood. The target-to-muscle ratio of ^{64}Cu-DOTA-anti-P-selectin mAb uptake in the aortic arch was significantly higher in *Ldlr*-/- mice fed with a high cholesterol diet than in those fed with normal chow (1.30 ± 0.07 vs. 0.22 ± 0.07; p <0.05). These data suggest that PET and CT fusion imaging demonstrates accumulation of ^{64}Cu-DOTA-anti-P-selectin mAb in the atherosclerosis-prone aortic root region in *Ldlr*-/- mice.

3.2. Ex vivo analysis of ^{64}Cu-DOTA-anti-P-selectin monoclonal antibody accumulation

Prior to the *ex vivo* study, we confirmed the accessibility of the anti-P-selectin antibody to the P-selectin in the plaques in aortas from *Ldlr*-/- mice fed with a high cholesterol diet by using immunofluorescence. As shown in the Supplementary data, the antibody specifically labels the P-selectin in the plaque.

To investigate probe accumulation in atherosclerotic plaques, Oil red O staining for lipid droplets and *ex vivo* autoradiography of aortas were performed after emission. Oil red O-stained atherosclerotic plaques were few in aortas from *Ldlr*-/- mice fed with normal chow (Fig. 2A). Accumulation of the probe was barely detectable in aortas by autoradiography in *Ldlr*-/- mice fed with normal chow (Fig. 2C). In contrast, Oil red O staining showed a prominent development of atherosclerotic plaques in the aortic root and major branches of *Ldlr*-/- mice fed with a high cholesterol diet (Fig. 2B). Autoradiographic images demonstrated uptake of the

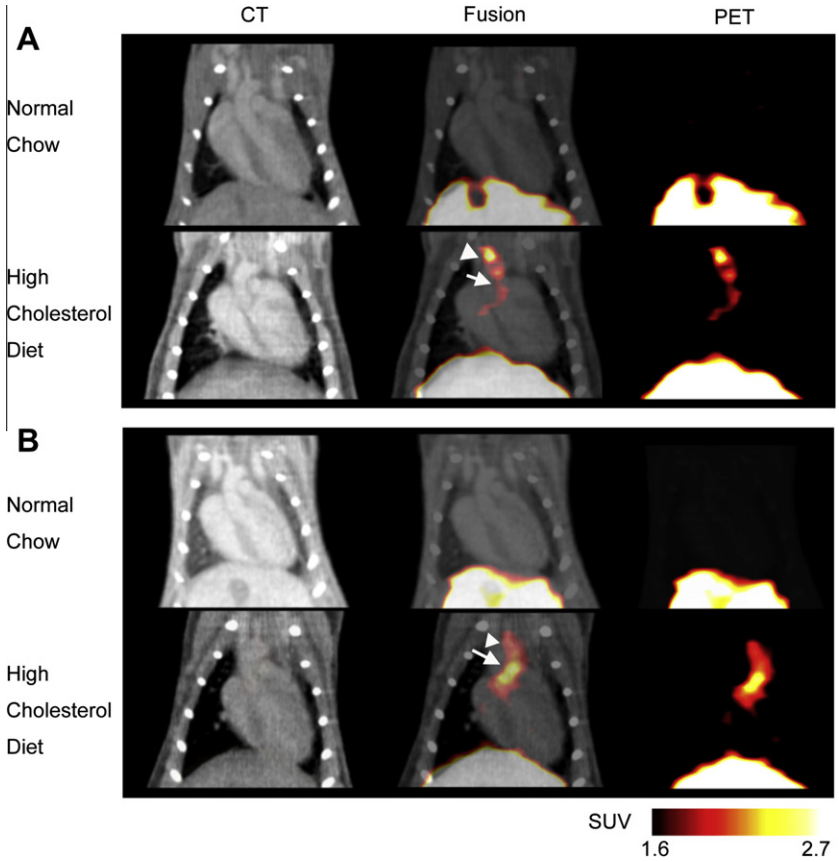

Fig. 1. PET and CT fusion images in *Ldlr*-/- mice. *In vivo* CT with contrast agent was performed 30 min prior to PET imaging for anatomical reference. *In vivo* PET imaging was performed for 180 min at 36 h after injection of ^{64}Cu-DOTA-anti-P-selectin mAb. CT (left), PET (right) and fusion (center; PET and CT co-registration) images of *Ldlr*-/- mice fed with normal chow (upper panels) and a high cholesterol diet (lower panels) are shown. (A) PET, CT and fusion images, injected with 3.0 MBq (0.017 nmol) of ^{64}Cu-DOTA-anti-P-selectin mAb. Arrowhead and arrow indicate prominent accumulation of ^{64}Cu-DOTA-anti-P-selectin mAb in the brachiocephalic artery and aortic arch, respectively. (B) PET and CT fusion images injected with 3.2 MBq (0.019 nmol) of ^{64}Cu-DOTA-anti-P-selectin mAb. Arrowhead and arrow indicate prominent accumulation of ^{64}Cu-DOTA-anti-P-selectin mAb in the brachiocephalic artery and ascending aorta, respectively.

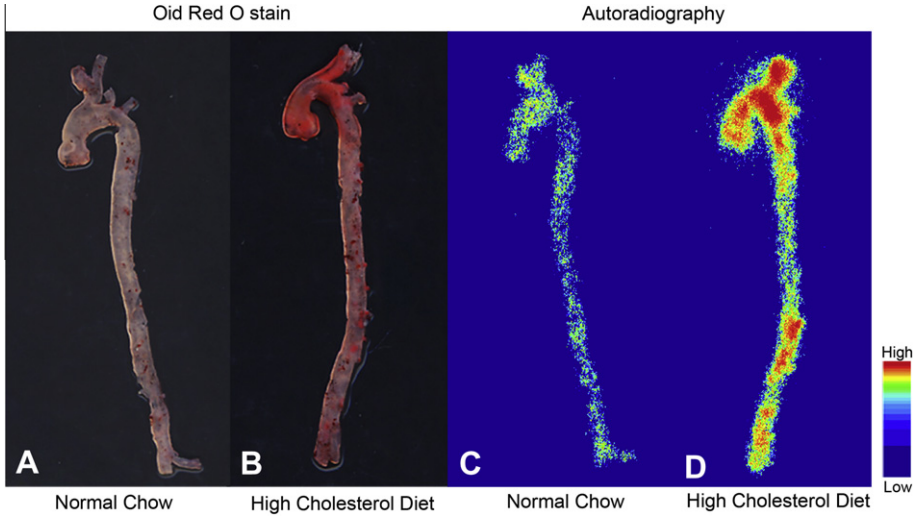

Fig. 2. ^{64}Cu-DOTA-anti-P-selectin mAb accumulates in atherosclerotic plaques. Aortas dissected after the PET scan from *Ldlr*-/- mice fed with normal chow (A and C) and a high cholesterol diet (B and D) were subjected to Oil red O staining followed by autoradiography. Representative photos of Oil red O stain (A and B) and autoradiography (C and D) are shown.

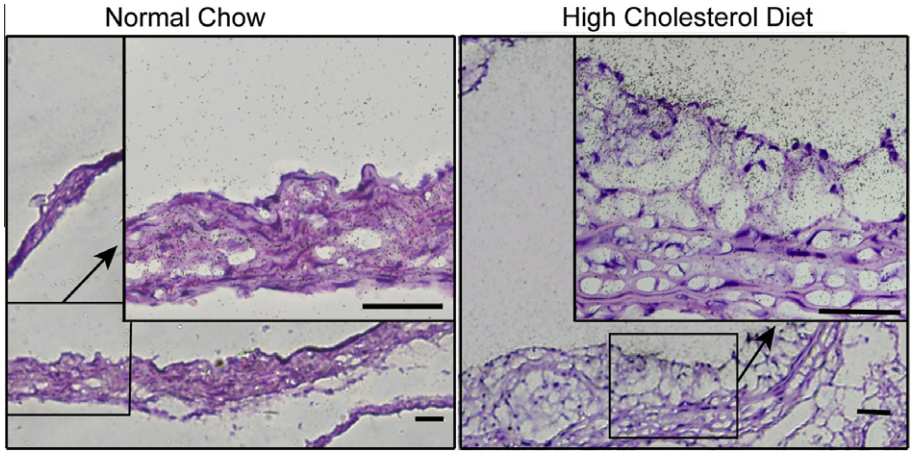

Fig. 3. Microautoradiography in aorta. Microautoradiography was performed after the PET scan to examine the fine localization of ^{64}Cu-DOTA-anti-P-selectin mAb in the aortic wall, followed by H&E staining. Representative images of microautoradiography combined with H&E staining of aortic sections from *Ldlr*-/- mice fed with normal chow and a high cholesterol diet are shown. The image depicted from the circled area is shown in the upper right corner of each panel. Bars, 50 μm.

probe into the region corresponding to atherosclerotic plaques indicated by Oil red O staining (Fig. 2D). These data suggest that the probe could show intense signals of accumulation in atherosclerotic plaques in *Ldlr*-/- mice fed with a high cholesterol diet.

3.3. Biodistribution of ^{64}Cu-DOTA-anti-P-selectin mAb

The biodistribution of ^{64}Cu-DOTA-anti-P-selectin mAb in tissues after emission was examined. The biodistribution of ^{64}Cu-anti-P-selectin mAb in the aorta was 6.6-fold higher in *Ldlr*-/- mice fed with a high cholesterol diet than that in *Ldlr*-/- mice fed with normal chow (8.05 ± 1.36%ID/g vs. 1.22 ± 0.23%ID/g, p <0.01). No significant differences in the biodistribution of ^{64}Cu-DOTA-anti-P-selectin mAb were found between mice fed with a high cholesterol diet as compared with mice fed with normal chow in the liver, spleen, kidney, skeletal muscle, fat and blood (liver, 15.7 ± 1.4 vs. 13.54 ± 0.60%ID/g; spleen, 12.39 ± 1.38 vs. 15.04 ± 1.8%ID/g; kidney, 5 ± 0.74 vs. 4.31 ± 0.26%ID/g; skeletal muscle, 0.54 ± 0.08 vs. 0.61 ± 0.15%ID/g; fat, 0.52 ± 0.11 vs. 0.87 ± 0.09%ID/g; blood, 4.63 ± 0.72 vs. 5.43 ± 0.59%ID/g, respectively; all comparisons not significant). These data suggest that ^{64}Cu-DOTA-anti-P-selectin mAb preferentially distributes in the aorta in *Ldlr*-/- mice fed with a high cholesterol diet when compared to that from *Ldlr*-/- mice fed with normal chow.

3.4. Microautoradiography in aorta

Microautoradiography was performed after emission to examine the fine distribution of ^{64}Cu-DOTA-anti-P-selectin mAb in the aortic wall. Atherosclerotic plaques and silver grain labeling were barely detectable in aortic sections from *Ldlr*-/- mice fed with normal chow (Fig. 3). In contrast, labeling with silver grains was observed in the *tunica intima* of atherosclerotic plaques identified by H&E staining of aortic sections from *Ldlr*-/- mice fed with a high cholesterol diet (Fig. 3). These data suggest that ^{64}Cu-DOTA-anti-P-selectin mAb can be used to detect the *tunica intima* of atherosclerotic plaques in *Ldlr*-/- mice.

4. Discussion

Coronary artery imaging using coronary arteriography and multidetector-row CT can provide useful information concerning the

morphology of coronary arteries in the clinical setting. Innovation of novel imaging methods with higher sensitivity and specificity for identification of atherosclerotic plaques is required for early stage detection of atherosclerotic plaques in increasing numbers of patients with coronary artery disease [1]. Combinations of pre-existing imaging methods have been suggested in order to improve the specificity of detection for atherosclerotic plaques in a non-invasive manner, and the present study aimed at imaging atherosclerotic plaques with PET and CT fusion imaging using an antibody-based probe designed to target a specific antigen.

Nonetheless morphological early stage detection, the progress in the understanding of the molecular basis of atherosclerosis has provided candidate antigens for antibody-based probes [14]. The leukocyte–endothelial interaction is mediated by adhesion molecules that are expressed on the cell surface of leukocytes and endothelial cells and are activated by atherogenic stimuli. This interaction occurs in the initial step of atherosclerosis, and it has been indicated that the adhesion molecules participating in the leukocyte–endothelial interaction are favorable targets for detection of atherosclerotic plaques during the earlier stages of atherosclerosis [14].

P-selectin expression has been shown to be upregulated in atherosclerotic plaques in mice and humans, and its functional significance in atherogenesis was demonstrated using P-selectin knockout mice [6,7,15]. Recent *ex vivo* as well as *in vivo* studies in mice showed that antibody-based probes for P-selectin and VCAM-1 that are adhesion molecules participating in the adhesion and recruitment of immune cells to arterial walls in atherosclerosis can be used to preferentially detect atherosclerotic plaques with ultrasound and MRI [16,17]. Accordingly, PET and CT fusion imaging of atherosclerotic plaques was investigated using an antibody-based probe in atherosclerosis-prone *Ldlr-/-* mice in the present study. Over the past decade, there have been a number of reports regarding targeting of particular cell membrane epitopes with monoclonal antibodies and receptors with radiolabeled peptides and peptidomimetics and imaging of the activity of particular enzymes and transporters. It is necessary for these probes to detect biological processes in lower concentrations without disturbing function [18]. In the present study, a ^{64}Cu-labeled antibody-based probe conjugated with DOTA was prepared with very high affinity to the antigen (K_d = 1.89 nM). Accumulation of the ^{64}Cu-DOTA-anti-P-selectin mAb in atherosclerotic plaques of the aorta and major branches in *Ldlr-/-* mice fed with a high cholesterol diet was observed by PET and CT fusion imaging followed by autoradiography and microautoradiography. A biodistribution study revealed preferential distribution of the probe in the atherosclerotic aorta. These data suggest that P-selectin is a suitable candidate of the target molecule(s) for imaging atherosclerosis plaques with PET and CT fusion imaging. A combination of molecular-targeting PET and CT could provide more specificity and higher spatial resolution to detect atherosclerotic lesions in mice, in comparison to other imaging modalities such as MRI and ultrasound. Further studies are necessary in other types of animal disease models to elucidate the usefulness of this atherosclerosis imaging.

Acknowledgments

We thank Drs. Yousuke Kanayama, Masanori Yamato and Yasuko Matsumoto of our center for their pertinent advice, and also thank Ms. Riyo Zochi, Ms. Emi Hayashinaka and Dr. Chinuyo Sumita for their skillful assistance. IN was supported by the Junior Research Associate Program, RIKEN. The funder had no role in study design, data collection and analysis, decision to publish, or preparation of the manuscript.

Appendix A. Supplementary data

Supplementary data associated with this article can be found, in the online version, at http://dx.doi.org/10.1016/j.bbrc.2013.02.069.

References

[1] U. Hoffmann, M. Ferencik, C.R. Ricardo Cury, J.A. Pena, Coronary CT angiography, J. Nucl. Med. 47 (2006) 798–806.
[2] P. Libby, Inflammation in atherosclerosis, Nature 420 (2002) 868–874.
[3] A.J. Lusis, Atherosclerosis, Nature 407 (2000) 233–241.
[4] C. Kneuer, C. Ehrhardt, M.W. Radomski, U. Bakowsky, Selectins – potential pharmacological targets?, Drug Discov Today 11 (2006) 1034–1040.
[5] E. Galkina, K. Ley, Vascular adhesion molecules in atherosclerosis, Atheroscler. Thromb. Vasc. Biol. 27 (2007) 2104–2112.
[6] R.R. Johnson-Tidey, J.L. McGregor, P.R. Taylor, R.N. Poston, Increase in the adhesion molecule P-selectin in endothelium overlying atherosclerotic plaques. Coexpression with intercellular adhesion molecule-1, Am. J. Pathol. 144 (1994) 952–961.
[7] R.C. Johnson, S.M. Chapman, Z.M. Dong, et al., Absence of P-selectin delays fatty streak formation in mice, J. Clin. Invest. 99 (1997) 1037–1043.
[8] A.M. Wu, Antibodies and antimatter: the resurgence of immuno-PET, J. Nucl. Med. 50 (2009) 2–5.
[9] M.R. Lewis, A. Raubitschek, J.E. Shively, A facile, water-soluble method for modification of proteins with DOTA. Use of elevated temperature and optimized pH to achieve high specific activity and high chelate stability in radiolabeled immunoconjugates, Bioconjugate Chem. 5 (1994) 565–576.
[10] Y. Ogawa, J. Traina, E. Zimmermann, T. Yu, D.W. Schneider, E. Pungor Jr., Quantification of bifunctional DTPA conjugation, Anal. Biochem. 368 (2007) 714–721.
[11] C.J. Anderson, J.M. Connett, S.W. Schwarz, et al., Copper-64-labeled antibodies for PET imaging, J. Nucl. Med. 33 (1992) 1685–1691.
[12] M. Iijima, H. Kadoya, S. Hatahira, et al., Nanocapsules incorporating IgG Fc-binding domain derived from *Staphylococcus aureus* protein-A for displaying IgGs on immunosensor chips, Biomaterials 32 (2011) 1455–1464.
[13] M. Yamato, Y. Kataoka, H. Mizuma, Y. Wada, Y. Watanabe, PET and macro- and microautoradiographic studies combined with immunohistochemistry for monitoring rat intestinal ulceration and healing processes, J. Nucl. Med. 50 (2009) 266–273.
[14] R.P. Choudhury, E.A. Fisher, Molecular imaging in atherosclerosis, thrombosis, and vascular inflammation, Atheroscler. Thromb. Vasc. Biol. 29 (2009) 983–991.
[15] G. Li, J.M. Sanders, E.T. Phan, K. Ley, I.J. Sarembock, Arterial macrophages and regenerating endothelial cells express P-selectin in atherosclerosis-prone apolipoprotein E-deficient mice, Am. J. Pathol. 167 (2005) 1511–1518.
[16] B.A. Kaufmann, C.L. Carr, J.T. Belcik, et al., Molecular imaging of the initial inflammatory response in atherosclerosis, Atheroscler. Thromb. Vasc. Biol. 30 (2010) 54–59.
[17] M.A. McAteer, K. Mankia, N. Ruparelia, et al., A leukocyte-mimetic magnetic resonance imaging contrast agent homes rapidly to activated endothelium and tracks with atherosclerotic lesion macrophage content, Arterioscler. Thromb. Vasc. Biol. 32 (2012) 1427–1435.
[18] M.E. Phelps, PET: the merging of biology and imaging into molecular imaging, J. Nucl. Med. 41 (2000) 661–681.